Sensors and Actuators B 133 (2008) 302–307

Contents lists available at ScienceDirect

Sensors and Actuators B: Chemical

journal homepage: www.elsevier.com/locate/snb

Characterization of gas sensing HfO_2 coatings synthesized by spray pyrolysis technique

A. Avila-García [a,*], M. García-Hipólito [b]

[a] CINVESTAV del I.P.N., Ingeniería Eléctrica, SEES, Sn. Pedro Zacatenco, G.A. Madero, México 07360, D.F., Mexico
[b] Universidad Nacional Autónoma de México, Instituto de Investigaciones en Materiales, Departamento de Materiales Metálicos y Cerámicos Ciudad Universitaria, Coyoacán, México 04510, D.F., Mexico

ARTICLE INFO

Article history:
Received 11 October 2007
Received in revised form 18 February 2008
Accepted 20 February 2008
Available online 29 February 2008

Keywords:
Hafnium oxide films
Gas sensors
Impedance response
Spray pyrolysis

ABSTRACT

Hafnium oxide (HfO_2) films were deposited using the ultrasonic spray pyrolysis deposition technique. The films were prepared using hafnium oxychloride as a raw material and deposited on Corning glass substrates at temperatures ranging from 300 °C to 500 °C. Their crystalline structure was dependent on the deposition temperature. At substrate temperatures below 350 °C the deposited films were almost amorphous, while at substrate temperatures higher than 400 °C the films became the monoclinic phase of HfO_2. Scanning electron microscopy and electron energy dispersion analysis showed a very rough surface with spherical particles of nearly stoichiometric HfO_2. Such films were assessed as active layers for humidity and propane sensors. Furthermore, their response characteristics calculated on the basis of the real and imaginary parts of the impedance and also on the total impedance value were determined as a function of the measurement frequency. The dynamic response to different concentrations of propane was obtained. The response and recovery times were also determined. Finally, a brief discussion on the possible sensing mechanisms was also presented.

1. Introduction

Hafnium oxide (HfO_2) films are deposited by a variety of techniques; these include atomic layer epitaxy [1], chemical vapor deposition [2], conventional electron beam evaporation [3], ion-assisted electron beam evaporation [4], sputtering [5], and ultrasonic spray pyrolysis [6]. Ultrasonic spray pyrolysis (USP) is a processing technique used in research to prepare thin and thick films and powders. Unlike many other film deposition techniques, USP represents a very simple and relatively cost-effective processing method (regarding equipment costs). It is a simple process for depositing films of any composition, specially oxides and sulphides. USP does not require high-quality substrates or chemicals. The method has been employed for the deposition of dense or porous films and for several types of powders production. Even multi-layered films can be easily prepared using this versatile technique. The precursor solutions used in this technique are obtained from inorganic and also organic salts such as chlorides, nitrates, acetates, acethylacetonates, ethoxides, butoxides, etc., dissolved in deionized water, alcohols or other organic solvents [7].

The transition metal oxides such as HfO_2 have received great attention because they are the materials with many potential applications. HfO_2 can be used for wave-guides [8], and for protective coatings due to its thermal stability and hardness [9,10]. Up to now one of the most important applications of this oxide is probably as a dielectric material with a relatively high dielectric constant and refractive index, and wide band-gap (E_g = 5.5–5.6 eV). These properties make it a good candidate for applications in metal-oxide semiconductor devices of the next generation [11,12]. The wide band-gap of HfO_2 makes it transparent over a wide spectral range: from the ultraviolet to the mid-infrared [4]. Then, HfO_2 has been employed in optical coating applications such as high-reflectivity mirrors, anti-reflection coatings, filters and beam splitters [13,14]. Also, the large-energy gap and low-phonon frequencies of the HfO_2 make it an appropriate host matrix for doping with rare-earth activators [15,6]. An incipient application to gas sensors has been proposed [16]. For this application, usage of transition metal oxides like HfO_2 is important due to the possibility of easily changing the metal oxidation states. There is a great demand for gas sensors to be used in various fields of industrial activity and as basic components in the monitoring of gas emissions and in control systems for pollution prevention and evaluation of air quality. Some of the available gas sensor devices, designed from semiconducting metal oxides, use the variation of the electrical conductivity of the oxide with the

* Corresponding author.
E-mail address: aavila@cinvestav.mx (A. Avila-García).

0925-4005/$ – see front matter © 2008 Elsevier B.V. All rights reserved.
doi:10.1016/j.snb.2008.02.031

composition of the gas in the surrounding atmosphere. Besides, considering that the process responsible for the change in electrical conduction takes place at the boundary between the gaseous and solid states, special attention must be paid to the surface features of the oxide [17]. The scientists have devoted considerable efforts to improving the properties of traditional sensors based on SnO_2, ZnO, TiO_2, and Fe_2O_3, hesitating to examine new metal oxides. Hafnium oxide films (both stoichiometric and pure) are usually insulators with an ionic conduction where the oxygen ions (O^{2-}) are the predominant moving species. Nevertheless, impurities, crystallographic defects, and mainly oxygen vacancies due to film preparation processes can generate intermediate states in the gap of the oxide, making it an n-type semiconductor. In this context the knowledge of the electronic transport properties of this material is very poor [16,17]. To our best knowledge, HfO_2 films have been only used as a gas sensor to detect CO gas and there are no reports, in literature, on this oxide as gas sensors for some other gases.

In this work HfO_2 coatings were synthesized by the USP technique, and their sensing characteristics to humidity and propane were studied. Also, the characteristics of the surface morphology, crystalline structure and chemical composition of the films are presented as a function of the deposition temperature.

2. Experimental details

The details of the USP technique have been described previously [18]. The starting reagent to deposit HfO_2 films was $HfOCl_2{\cdot}8H_2O$. The initial solution was 0.7 M in deionized water. Deposition temperatures (T_s) were in the range from 300 °C to 500 °C. Corning glass pieces of 1 cm × 1.5 cm were used as substrates. The carrier gas was filtered air and the flow rate was 8 l/min. The deposition time was 5–6 min for all the samples in order to reach films with almost the same thickness. This thickness was approximately 12 μm as measured by a Sloan Dektak IIA profilometer (within ±0.03 μm). Microstructure and elementary composition measurements were carried out on a Cambridge–Leica scanning electron microscopy (SEM) model stereoscan 440 by means of energy dispersive spectroscopy (EDS) with an X-ray detector of Si–Li Oxford model Pentafet. X-ray diffraction (XRD) was used to analyze the crystalline structure by means of a Siemens D-5000 diffractometer with Cu Kα radiation (λ = 1.5406 Å). The alternating current measurements were carried out with an SR830 DSP Lock-In amplifier by using its sinusoidal internal signal as the measurement signal and determining from the input in-phase and in-quadrature voltages the impedance of the samples. The frequency range was from 1 Hz to 10^5 Hz. The small signal was almost always 15 mV rms in amplitude, but sometimes 50 mV and even 2.5 V were needed to overcome the high impedance values of the samples. The sample was introduced into a small chamber (approximately of 133 cm^3 volume) with a controlled temperature basement. By opening and closing the appropriate valves of the gas feeding system the inner atmosphere can be changed. Three types of atmosphere were used: zero grade air (80% nitrogen and 20% oxygen), zero grade air plus humidity (~53% R.H.) and zero grade air plus humidity plus some amount of propane (189 ppm, 500 ppm and 786 ppm). In order to reproduce work conditions, the electrical measurements were performed at near atmospheric pressure.

3. Results and discussion

In Fig. 1, the results of XRD measurements carried out on HfO_2 films are shown. Diffraction patterns of samples deposited at T_s from 300 °C to 500 °C are exhibited. Coatings grown at low deposition temperatures (300 °C and 350 °C) have poor crystallinity, so they can be considered as amorphous and/or nanocrystalline layers. For higher T_s, the films show the characteristic peaks of the hafnium oxide monoclinic phase (referenced JCPDS 431017). Sharper diffraction peaks at high T_s could indicate an increase of the crystallites size. The XRD spectra revealed a preferential (1 1 1) orientation of HfO_2 normal to the films surface.

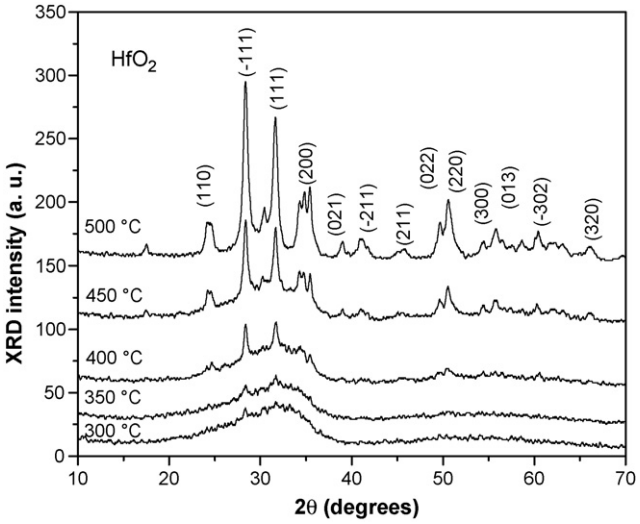

Fig. 1. XRD diffractograms for HfO_2 films grown at different T_s: 300 °C, 350 °C, 400 °C, 450 °C and 500 °C.

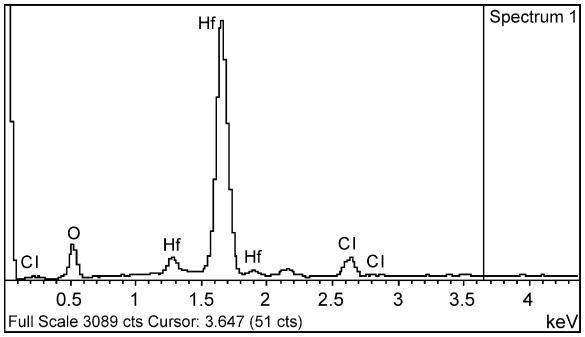

Fig. 2. EDS pattern for an HfO_2 film deposited at 500 °C, showing its basic composition. Peaks evidencing the presence of hafnium, oxygen and chlorine are clearly seen.

An EDS spectrum is shown in Fig. 2. It clearly shows that Hf, O and Cl are included in the film deposited at 500 °C. A comparison of the results from the samples deposited at different temperatures is shown in Table 1. It summarises the relative atomic percentages of oxygen, chlorine and hafnium contained in the films as a function of the deposition temperature. It is possible to observe that the relative content of oxygen is maintained constant, the hafnium relative content is slightly increased and in the relative content of chlorine

Table 1
Atomic percent content of oxygen, chlorine and hafnium inside hafnium oxide films as determined by EDS for different substrate temperatures

T_s (°C)	O	Cl	Hf
300	62.0	8.0	30.0
350	63.2	6.7	30.1
400	64.1	4.8	31.1
450	63.0	4.1	32.9
500	63.5	3.0	33.5

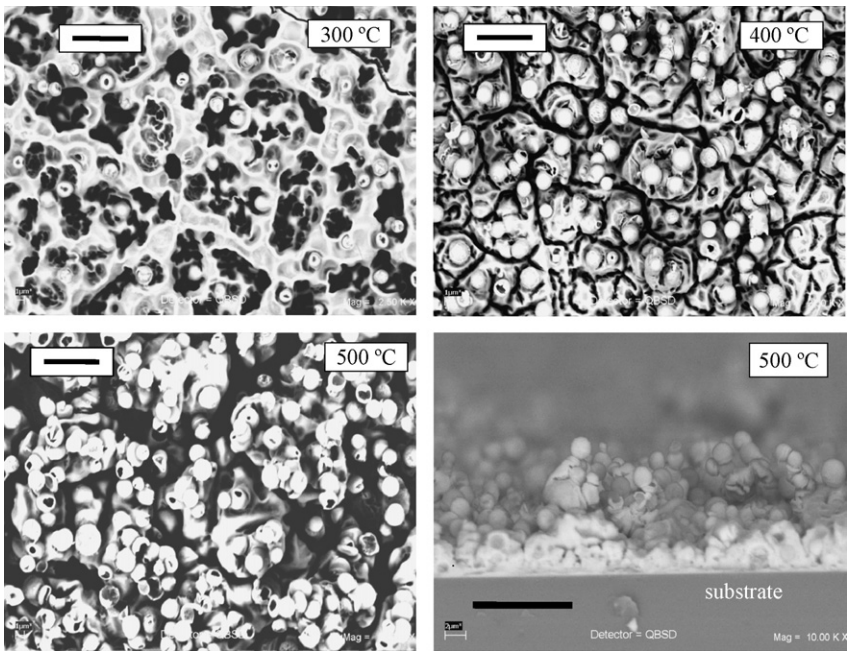

Fig. 3. SEM micrographs of surface morphology of HfO_2 coatings as a function of T_s: 300 °C, 400 °C, 500 °C and cross-section of the sample deposited at 500 °C. The length of the black bars represents 10 μm.

is appreciable reduced, as the deposition temperature increases. The films, in general, are oxygen deficient.

In Fig. 3 SEM micrographs of the surface morphology of the coatings are presented. It is possible to observe rough and continuous films with good adherence to the substrate. No specific adherence proof was done, but none of the films lifted up after manipulation during the different measurements performed. Samples deposited at 300 °C, 400 °C, 500 °C and a cross-section of that deposited at 500 °C are shown in this figure. The surface morphology of the films depends on the deposition temperature. The film deposited at 300 °C presents a rough and porous surface with a few spherical particles. The coating deposited at 400 °C presents a more compact surface than that deposited at 300 °C (with a larger quantity of apparently solid spherical particles). As the deposition temperature increases (500 °C), a rough surface with a more open network is observed; in this case most of the spherical particles are exploited, which produces a film with a higher superficial area. These characteristics are probably obtained because at higher substrate temperature the deposited precursors have larger surface kinetic energy, which produces a more complete pyrolytic reaction of the reactant materials. In addition, a cross-section of the sample deposited at 500 °C is exhibited. Here it is possible to observe a nodular growth of the film further than a columnar one. It is possible to observe that the coating is formed by two sections: one is composed of a solid layer of approximately 0.5–1 μm (white region) and above this one, a porous section of about 11 μm (grey area) composed of spherical particles of diverse sizes (typically 1–2 μm). Also, the thickness here observed is similar to the value measured by the profilometer.

Alternating current measurements at 30 °C and 250 °C were carried out. Impedance values ($Z = Z' + iZ''$) of the samples are determined in the various atmospheres aforementioned as a function of the frequency. After performing such measurements, the corresponding results can be presented in several forms. A compact form was proposed by Macdonald et al. [19]. They consider the imaginary part Z'' as a 3D line function of the real part Z' and the frequency f. Then, the projections of this 3D line on the coordinate planes provide the frequency dependence of Z' and Z'' besides the Z'' vs. Z' plot. Measurements only for the film grown at 500 °C are presented here. In Fig. 4 the projections on the coordinate planes above mentioned within the three atmospheres of this work are shown. The 3D line is not included for the sake of clearness. The curves in Fig. 4a were obtained at 30 °C with 2.5 V rms due to the high impedance of the sample. Those of Fig. 4b were measured at 250 °C with 15 mV rms because the impedance decreases at higher temperature. In these figures 'D' stands for "dry air", 'H' for "humid air" and 'HP' for "humid air + 500 ppm propane". The most noticeable effects after changing the atmosphere are seen to happen at 30 °C in Fig. 4a. A large effect is clearly seen on the imaginary part Z'' of the impedance and occurs at low frequencies. At 250 °C the largest changes are again produced on Z'' at low frequencies, but they are smaller than those at 30 °C. A capacitive equivalent circuit can be ascribed to the impedance plots depicted in Fig. 4. The magnitudes of Z' and Z'' are much larger in Fig. 4a than in b, due to the difference of temperature. Furthermore, in Fig. 4b the smaller magnitudes allow to resolve two contributions to the impedance of the sample. These are seen as two separate semi-circles. The larger resistance and reactance changes produced at low frequencies by both humidity and propane are presumably related to the surface contribution to the film impedance [20,21].

The qualitative observations above made can be measured by defining the response to both humidity and propane. We are interested only on the magnitude of the difference of either Z', Z'' or Z produced after changing the atmosphere. Then, the definition we use to calculate the sensor response in percentage is given by the expression:

$$S_{H,P}(X) = \left| \frac{X_{H,HP}}{X_{D,H}} - 1 \right| \times 100 \quad (1)$$

where X stands for Z', Z'' or Z. In this expression, for the case of response to humidity, the subscript H in the left-hand side is used together with H in the numerator of the right-hand side and D on the denominator. For the response to propane, the remaining subscripts are used.

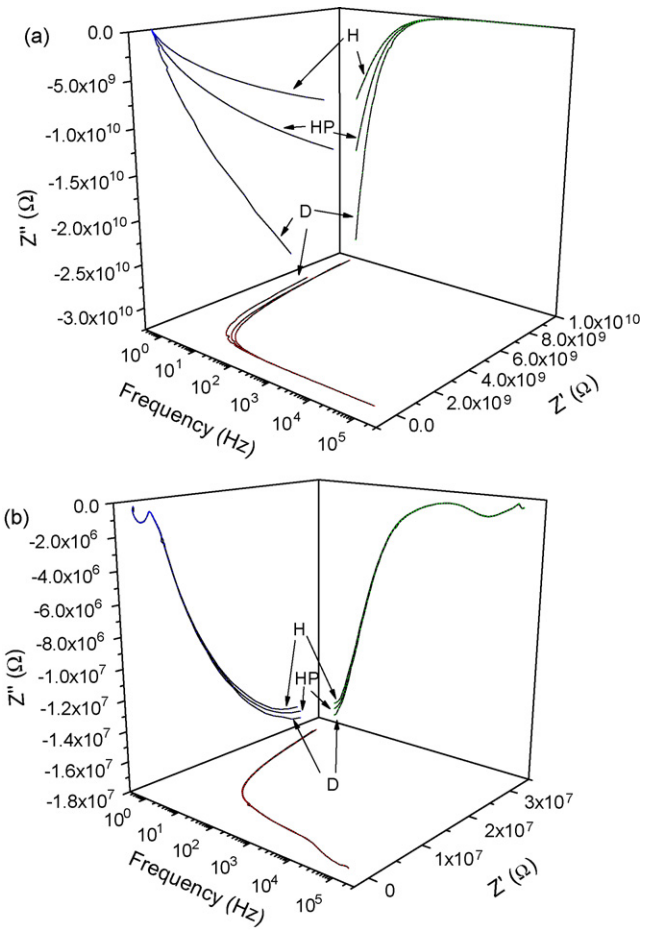

Fig. 4. Simultaneous plotting of the Z' and Z'' dependence on measurement frequency and Z'' vs. Z'. The 3D line curves whose projections are the graphs shown here are not depicted for the sake of clearness: (a) results under dry air (D), humid air (H) and humid air plus 500 ppm propane (HP) at 30 °C and (b) results at 250 °C.

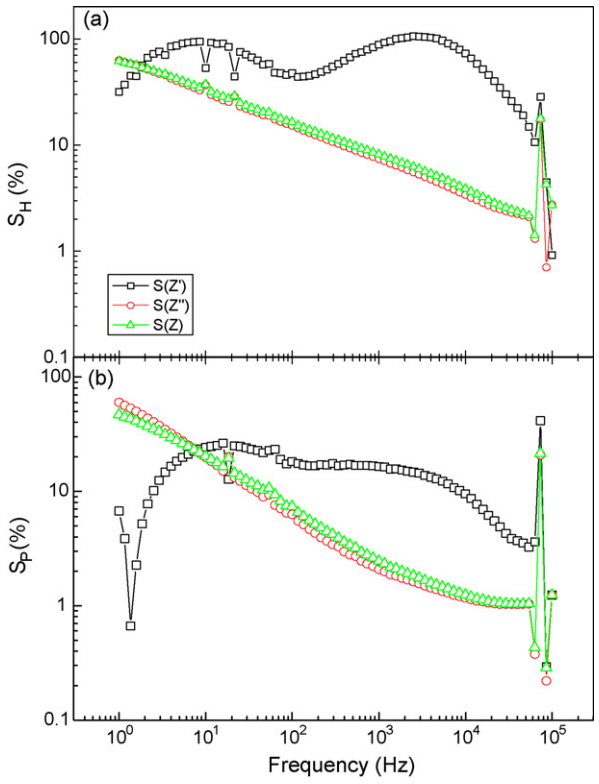

Fig. 5. Percentage responses as a function of measurement frequency calculated from Eq. (1): (a) responses based on Z', Z'' and Z to humidity at 30 °C and (b) to propane at 30 °C.

After using the last formula for Z', Z'' and Z as a function of frequency, the plots of Fig. 5 were obtained for the measurements at 30 °C.

Two relative maxima around 100% of the resistive response to humidity near 6 Hz and 3 kHz can be seen in Fig. 5a. Instead, in the same figure a decreasing trend can be observed for the reactive response, which behaves quite similarly to the total impedance response. Hence, the maximum response around 60% in this case corresponds to frequencies near 1 Hz. The peaked responses near 100 kHz are related to some resonant nature of the sample that is left for later study.

As expected from Fig. 4b, at 250 °C response values lower than 6% turned out to both humidity and propane, so they are not illustrated. In this respect, the behavior of HfO_2 films towards water is similar to that of SnO_2 pellets [22], exhibiting a high response at low temperature and a poor response at 250 °C. At low temperature the response is associated to reversible molecular water adsorption that provides a parallel conduction path. At 250 °C the response is ascribed to hydroxyl species coming from water reaction. However, at this temperature hydroxyl species tend to be irreversibly bound, hence a poor reversible response is observed. According to Norris [22], the response to hydrocarbons is largely determined by adsorbed moisture.

Regarding the distinct responses to propane at 30 °C that was based on the resistive nature of the sample has a relative maximum of about 25% at near 20 Hz. The reactive response is again very similar to the total impedance response and decreases from a maximum of about 60% at 1 Hz downwards 1% at about 50 kHz.

The dynamic responses of Z' and $-Z''$ to several concentrations of propane within humid air (approximately 53% R.H.) are plotted in Fig. 6. They were obtained at 30 °C and 100 Hz frequency. Also shown is the propane concentration. Both signals are measured during 5 min at the beginning. Then 10 min long pulses of 189 ppm, 500 ppm and 786 ppm are alternated with zero concentration also along 10 min to allow for recovery of the sample. It is seen that both Z' and Z'' decrease under the effect of propane on the

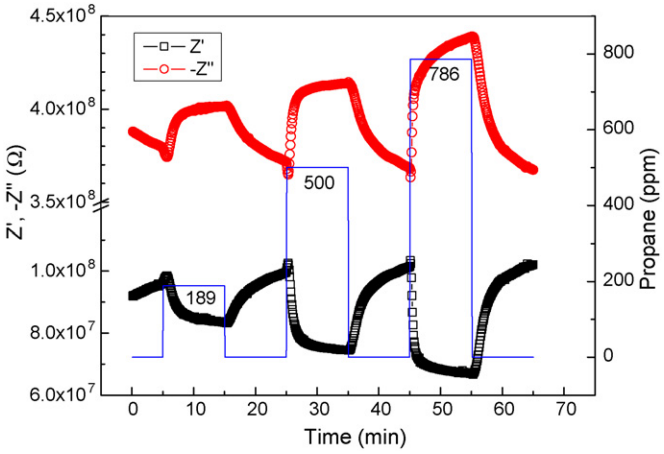

Fig. 6. Dynamic response of Z' and $-Z''$ of the sample grown at 500 °C under the effect of different size of propane pulses. The amplitude and frequency of the measurement signal were 2.5 V rms and 100 Hz, respectively. The sample was measured at 30 °C.

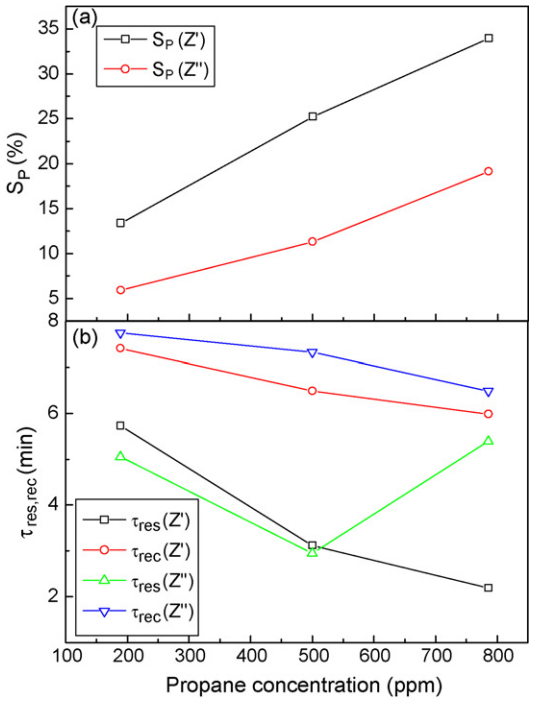

Fig. 7. (a) Responses of both Z' and Z'' as a function of the propane concentration, showing reasonable linearity; (b) response and recovery times of Z' and Z''.

film and certainly the total change produced after 10 min depends on the concentration of propane. The recovery value is similar after the three pulses of propane. Information on the linearity of both responses and also on the response and recovery times is provided after a detailed analysis of these plots. These are the times needed to reach 90% of the total change after the cycling time of 10 min. Such results depend on the propane concentration, as shown in Fig. 7. In Fig. 7a reasonable linearity of the Z' and Z'' responses turns out for the propane concentration range from 189 ppm to 786 ppm. Also, better responses to propane ranging from 13% up to 34% are achieved by the real part of the impedance for all concentration values. The reactive response value goes only from 6% up to 19%. In Fig. 7b the recovery time τ_{rec} of both Z' and Z'' is seen to be longer than the corresponding response time τ_{res} for all the propane concentrations. It ranges from 6 min to 8 min in both cases and behaves decreasingly with propane concentration. Instead, the response time goes from near 2 min to less than 6 min. The resistive response behaves again decreasing with concentration, but the reactive response decreases from 189 ppm to 500 ppm and then increases again up to near 6 min at 786 ppm. This reactive response is of capacitive type, necessarily related to charge storage processes resulting from the gas–surface interaction. The slowing of reactive response with a propane increase could be related to the surface morphology if it is accepted that the compact region of the film reacts slowly with the gas and the porous region reacts faster. The first region which reacts with the gas is that with protruding shells upon the surface, but as the gas concentration increases, a larger contribution from the compact region could be involved, then requiring longer times for the whole effect.

A similar chemical process for the interaction of CO with HfO_2 to that with SnO_2 has been formerly proposed [16]. As noted formerly, HfO_2 and SnO_2 behave similarly at 30 °C and 250 °C under the effect of water. On the other hand, the Mars–van Krevelen redox mechanism is generally accepted as the first step in the cases of alkane oxidation reactions with metal oxides [23,24]. The second step is re-oxidation by O_2 at the surface [24]. The behavior of the resistive response is carefully studied and explained by Koziej et al. [23] by using simultaneously several experimental techniques. They conclude that propane dissociates on acid–base pair sites forming propyl radicals, which in turn react with adsorbed oxygen species. As a result, ionic carboxylates and carbonates are produced which are lately degraded to $CO_{2(g)}$ and $H_2O_{(g)}$ only.

Response of HfO_2 films to 786 ppm propane is of the same order as that reported for tin oxide films to 3000 ppm propane [25].

4. Conclusions

This contribution reports on the structural, morphological and humidity and propane sensing characteristics of HfO_2 films which are synthesized by the USP process. These films show good adherence to the substrate and a high-deposition rate up to 2 μm min^{-1}. The crystalline structure of the analyzed coatings depended on the substrate temperature; at low temperatures (300–350 °C) they are in an amorphous state and when the deposition temperature is increased they are transformed, mainly, to a polycrystalline monoclinic HfO_2 phase. Also, the surface morphology of the coatings was dependent on T_s, SEM micrographs showed that these films were very rough with spherical particles on the surface. Significant response of the films to both humidity and propane was obtained at 30 °C but not at 250 °C. Some response at a different high-temperature value cannot be discarded. The electrical measurements were done at practically atmospheric pressure. At 30 °C, the maximum resistive response of the films to humidity was up to 100%, depending on the measurement frequency. On the other hand, the maximum reactive response was about 60%. Regarding propane, the resistive response was only about 25% while the reactive one was 60%. The response times were always less than 6 min and the recovery times were less than 8 min, depending on the propane concentration. The chemical response mechanism to propane proposed for HfO_2 is similar to that formerly given for SnO_2. Also, a slightly higher response to propane is determined for HfO_2 than that known for SnO_2.

Acknowledgments

The authors thank L. Baños for XRD measurements, J. Guzmán-Mendoza for SEM images, and Enriqueta Aguilar-Valencia for technical support.

References

[1] M. Ritala, M. Leskela, L. Niinisto, T. Prohaska, G. Friedbacher, M. Grasserbauer, Development of crystallinity and morphology in hafnium dioxide thin films grown by atomic layer epitaxy, Thin Solid Films 250 (1994) 72–80.
[2] M. Balog, M. Schieber, M. Michman, S. Patai, Chemical vapor deposition and characterization of HfO_2 films from organo-hafnium compounds, Thin Solid Films 41 (1977) 247–259.
[3] D. Reicher, P. Black, K. Jungling, Defect formation in hafnium dioxide thin films, Appl. Opt. 39 (2000) 1589–1599.
[4] J. Lehan, Y. Mao, B.G. Bovard, H.A. Macleod, Optical and microstructural properties of hafnium dioxide thin films, Thin Solid Films 203 (1991) 227–250.
[5] Y.J. Cho, N.V. Nguyen, C.A. Richter, J.R. Ehrstein, B.H. Lee, J.C. Lee, Spectroscopic ellipsometry characterization of high-*k* dielectric HfO_2 thin films and the high-temperature annealing effects on their optical properties, Appl. Phys. Lett. 80 (2002) 1249–1251.
[6] M. García-Hipólito, U. Caldiño, O. Alvarez-Fragoso, M.A. Alvarez-Pérez, R. Martínez-Martínez, C. Falcony, Violet–blue luminescence from hafnium oxide layers doped with $CeCl_3$ prepared by the spray pyrolysis process, Phys. Stat. Sol. (A) 204 (2007) 2355–2361.
[7] D. Perednis, L.J. Gauckler, Thin film deposition using spray pyrolysis, J. Electroceram. 14 (2005) 103–111.
[8] A. Waldorf, J.A. Dobrowolski, B.T. Sullivan, L.M. Plante, Optical coatings deposited by reactive ion plating, Appl. Opt. 32 (1993) 5583.
[9] H. Ibégazéne, S. Alpérine, C. Diot, Yttria-stabilized hafnia–zirconia thermal barrier coatings: the influence of hafnia addition on TBC structure and high-temperature behaviour, J. Mater. Sci. 30 (1995) 938–951.

[10] J. Wang, H.P. Li, R. Stevens, Hafnia and hafnia-toughened ceramics, J. Mater. Sci. 27 (1992) 5397–5430.
[11] G.D. Wilk, R.M. Wallace, J.M. Anthony, High-*k* gate dielectrics: current status and materials properties considerations, J. Appl. Phys. 89 (2001) 5243–5275.
[12] L. Niimistö, J. Päiväsaari, J. Niimistö, M. Putkonen, M. Nieminen, Advanced electronic and optoelectronic materials by atomic layer deposition: an overview with special emphasis on recent progress in processing of high-*k* dielectrics and other oxide materials, Phys. Stat. Sol. (A) 201 (2004) 1443–1452.
[13] M. Zukic, D.G. Torr, J.F. Spann, M.R. Torr, Vacuum ultraviolet thin films. 1. Optical constants of BaF_2, CaF_2, LaF_3, MgF_2, Al_2O_3, HfO_2, and SiO_2 thin films, Appl. Opt. 29 (1990) 4284–4292.
[14] S.M. Edlou, A. Smajkiewicz, G.A. Al-Jumaily, Optical properties and environmental stability of oxide coatings deposited by reactive sputtering, Appl. Opt. 32 (1993) 5601–5605.
[15] S. Lange, V. Kiisk, V. Reedo, M. Kirm, J. Aarik, I. Sildos, Luminescence of RE-ions in HfO_2 thin films and some possible applications, Opt. Mater. 28 (2006) 1238–1242.
[16] S. Capone, G. Leo, R. Rella, P. Siciliano, L. Vasanelli, M. Alvisi, L. Mirenghi, A. Rizzo, Physical characterization of hafnium oxide thin films and their application as gas sensing devices, J. Vac. Sci. Technol. A 16 (1998) 3564–3568.
[17] S.M.A. Durrani, CO-sensing properties of hafnium oxide thin films prepared by electron beam evaporation, Sens. Actuators B 120 (2007) 700–705.
[18] M. Langlet, J.C. Joubert, in: C.N.R. Rao (Ed.), Chemistry of Advanced Materials, Blackwell Science, Oxford, England, 1993, p. 55.
[19] J.R. Macdonald, J. Schoonman, A.P. Lehnen, Three dimensional perspective plotting and fitting of immittance data, Solid State Ionics 5 (1981) 137–140.
[20] U. Weimar, W. Göpel, A.c. measurements on tin oxide sensors to improve selectivities and sensitivities, Sens. Actuators B 26–27 (1995) 13–18.
[21] G. Neri, A. Bonavita, S. Galvagno, N. Donato, A. Caddemi, Electrical characterization of Fe_2O_3 humidity sensors doped with Li^+, Zn^{2+} and Au^{3+} ions, Sens. Actuators B 111–112 (2005) 71–77.
[22] J.O.W. Norris, in: P.T. Moseley, B.C. Tofield (Eds.), The Role of Precious Metal Catalysts in Solid State Gas Sensors, Adam Hilger, Bristol/Philadelphia, 1987, p. 124.
[23] D. Koziej, N. Bârsan, V. Hoffmann, J. Szuber, U. Weimar, Complementary phenomenological and spectroscopic studies of propane sensing with tin dioxide based sensors, Sens. Actuators B 108 (2005) 75–83.
[24] C.N. Satterfield, Heterogeneous Catalysis in Industrial Practice, McGraw-Hill, 1991.
[25] S.K. Song, J.S. Cho, W.K. Choi, H.J. Jung, D. Choi, J.Y. Lee, H.K. Baik, S.K. Koh, Structure and gas-sensing characteristics of undoped tin oxide thin films fabricated by ion-assisted deposition, Sens. Actuators B 46 (1998) 42–49.

Biographies

Alejandro Avila-García received the MSc degree in solid-state electronics from CINVESTAV-IPN in 1983 and also the MSc degree in physics and technology of amorphous materials from the University of Dundee in 1986. Then, he obtained the Dr. degree in solid-state electronics from CINVESTAV-IPN in 1997. He is currently a researcher and lecturer in the Department of Electrical Engineering of CINVESTAV-IPN since 1987. His current interest is on the fabrication and characterization of semiconductor and metal oxide films for different applications, such as gas sensors, selective surfaces and active layers in solar cells and other devices.

M. García-Hipólito was graduated from the Faculty of Sciences (Physics) of the University of México (UNAM) in 1986 and continued his post-graduate studies in the National Polytechnic Institute of México. In 2003 he received his PhD degree from this institution in advanced technology. From 1986 he has been working in the Institute of Investigations in Materials, UNAM on the synthesis (by spray pyrolysis, sputtering, PECVD, sol–gel and thermal evaporation techniques) of materials (films and powders) such as semiconductors and insulators and its morphological, structural, optical and electrical characterization. Also, his research interests include the luminescent characteristics of the materials above-mentioned.